ChemComm

Accepted Manuscript

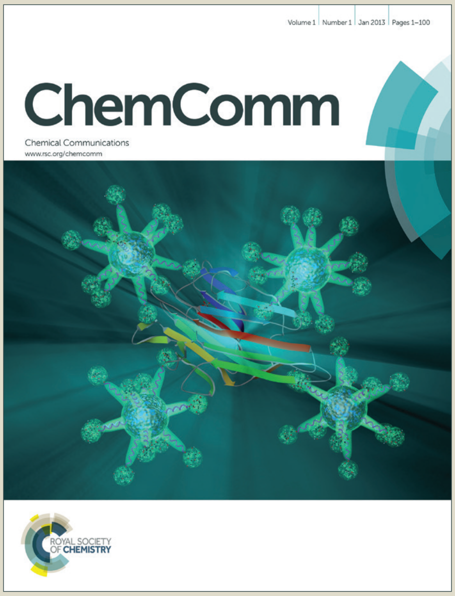

ROYAL SOCIETY OF CHEMISTRY

www.rsc.org/chemcomm

Chemical Communications RSCPublishing

COMMUNICATION

Synthesis of Organic Charge Transfer Hetero-Microtubules by Crack Welding

Cite this: DOI: 10.1039/x0xx00000x

J. Kim,[a] J. Chung,[a] J. Hyon,[a] T. Kwon,[a] C. Seo,[a] J. Nam,[a] Y. Kang[a]*

Received 00th January 2012,
Accepted 00th January 2012

DOI: 10.1039/x0xx00000x

www.rsc.org/

The strain-induced cracks in organic microtubules composed of an organic charge transfer (CT) complex of 1,2,4,5-tetracyanobenzene (TCNB) and naphthalene were selectively welded via the formation of secondary CT complexes; this process, in turn, led to the formation of organic hetero-microtubules consisting of multiple segments of two organic CT complexes.

The synthesis of heterogeneous microstructures or nanostructures with desirable spatial organizations is important for creating multifunctional materials.[1] The integration of dissimilar multiple constituents within a confined geometry often leads to unique chemical and physical properties by synergistic coupling of each component, whereas such properties are not usually observed in the case of homogeneous materials.[1f,2] Because of their unique properties, heterogeneous structures have been used in various engineering applications in the field of solar cells,[3] photocatalysis,[4] electronics,[5] optics,[1h,6] and biomedical imaging.[7] The preparation of hetero-nanostructures often involves the sequential growth of each component by self-assembly[5c,8] or by template-directed synthesis.[9] Although these synthesis methods can be applied to a wide range of combinations of inorganic materials, the choice of appropriate organic material pairs is quite limited and the desired heterogeneous nucleation competes with homogeneous nucleation, which often leads to the formation of secondary homogeneous particles. Doping or ion-exchange methods were introduced as an alternative approach to create heterogeneous structures while avoiding separate nucleation.[10] Although some inorganic heterogeneous nanostructures have been prepared by doping or ion-exchange methods,[10a,11] similar syntheses of organic heterogeneous nanostructures have rarely been reported.[12]

Herein, we report an approach to fabricate organic heterogeneous microtubular structures consisting of multiple segments of charge transfer (CT) complexes by the "crack-welding" (Scheme 1) method. Our method exploits the selective doping and growth of secondary CT complexes at strain-induced cracks in microtubular CT complexes. The cleaved facets normal to the growth direction inevitably have a higher surface energy than other facets, and they can be utilized as nucleation sites for the selective doping and growth of secondary materials.[13] Herein, we intentionally generated cracks in the microtubules and selectively grew secondary CT complexes on the cleaved edges to yield organic hetero-microtubules exhibiting dual emission colors. To exemplify our idea, we prepared microtubules using 1,2,4,5-tetracyanobenzene (TCNB) and naphthalene (NAP) CT complex and then selectively grew secondary CT complexes on the cleaved facets of the microtubules by sublimating aromatic dopants, such as pyrene (PY), 9-methylanthracene (9MA), and phenanthrene (PNT) onto the microtubules. Although some solution growth methods have been reported for the growth of microtubular CT complexes based on TCNB,[12,14] we developed a novel eutectic-melting-assisted soft-lithography method to facilitate the formation of cracks in the CT microtubules.

Scheme 1. Fabrication of organic CT hetero-microtubules via the "crack-welding" method

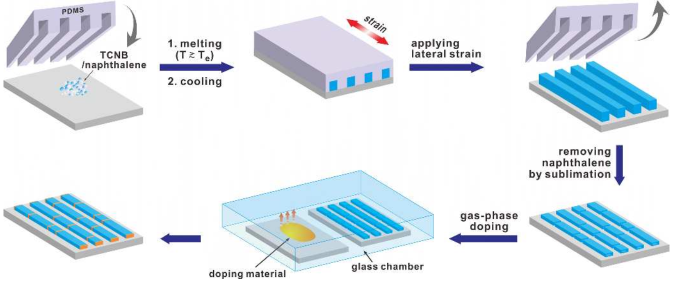

The electron-deficient TCNB is known to form stable CT complexes with various aromatic hydrocarbon compounds.[12,14] In our experiments, NAP was chosen not only because it forms a good CT complex with TCNB but also because it forms good eutectic mixtures with various organic solids, including TCNB. We recently developed a melting crystallization method that utilizes eutectic mixtures. A microtubular TCNB–NAP CT complex can be easily prepared by our eutectic melting method at a moderately low temperature. The microtubules shown in Figure 1a were prepared by eutectic melting/crystallization. First, TCNB and NAP powders were mixed in a ratio of 2:8. After they were finely pulverized, the mixtures were melted at 80 °C, which is slightly higher than the eutectic temperature (T_e = 72 °C) of TCNB and NAP (Figure S1). The samples were saturated with NAP vapor during the melting process to prevent significant composition changes. After the mixtures completely melted, they were immediately cooled to room temperature. Finally, the TCNB–NAP CT complex was isolated by sublimation of the residual NAP. Because the vapor pressure of the CT complexes are significantly lower than that of NAP, the unreacted NAP can be easily removed by sublimation under mild vacuum conditions at room temperature without disturbing the structures of the formed CT complexes. As shown in Figure 1d, the isolated TCNB–NAP CT complex crystallized in the shape of a rectangular microtubule with a length of several hundred micrometers and a width of several micrometers. The shape of the microtubules prepared by our method is very similar to that of microtubules prepared by the typical solution growth method, as reported elsewhere.[12,14b] The microtubules exhibited strong blue emission under UV irradiation, which strongly suggests that the TCNB–NAP CT complex was formed by the eutectic melting/crystallization method (Figure 1). The PL spectrum of the TCNB–NAP microtubules showed a broad band at λ_{max} = 487 nm, which is associated with a charge transition from the highest occupied molecular orbital (HOMO) of NAP to the lowest unoccupied molecular orbital (LUMO) of TCNB.[14c,15] The TCNB–NAP microtubules could be homogeneously doped by the addition of small amount of the secondary aromatic hydrocarbon compounds during the eutectic melting/crystallization process. Figure 1b shows the TCNB–NAP microtubules doped with PY. Whereas their shape and dimensions were same as those of the TCNB–NAP microtubules, the PL peak shifted to a longer wavelength corresponding to their exhibition of an orange color (λ_{max} = 569 nm). This shift indicates the formation of the TCNB–NAP–PY CT complex.[14b]

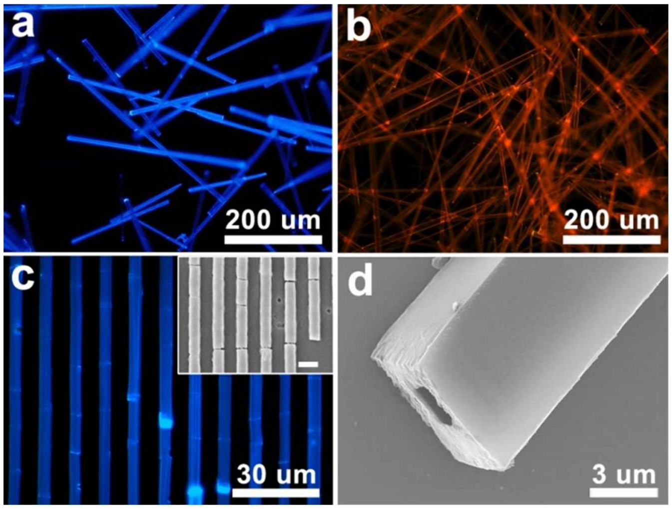

Figure 1. Fluorescence microscope images of a) TCNB–NAP and b) TCNB–NAP–PY microtubules prepared by eutectic melting/crystallization. c) Fluorescence microscope image of TCNB–NAP microtubules prepared by eutectic-melting-assisted soft-lithography. The cracks in the microtubules were generated by applying axial strains on the PDMS mold during the μTM process. The inset SEM image shows that numerous cracks were formed normal to the growth direction of the microtubules. The scale bar in the inset is 10 μm. d) SEM image of a TCNB–NAP microtubule.

Because TCNB and NAP mixtures melt at low temperatures (T_e = 72 °C) without damaging polydimethylsiloxane (PDMS), a conventional material for soft-lithography, the micro-transfer molding (μTM) technique was applicable for creating microtubule patterns. As illustrated in Scheme 1, a TCNB and NAP mixture was first melted onto silicon wafer at 80 °C while covered with a PDMS mold. The sample was subsequently cooled to the room temperature, and a small amount of uniaxial strain ($\varepsilon \approx 5\%$) was applied to the PDMS mold along the pattern axis.

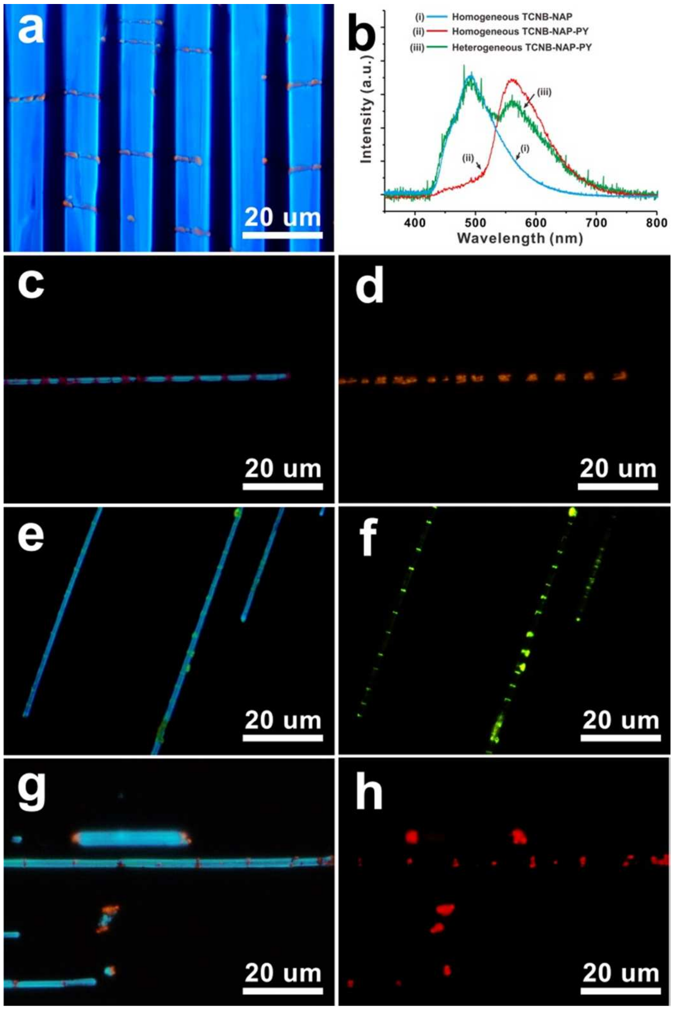

Figure 2. a) Fluorescence microscope image of TCNB–NAP–PY hetero-microtubules exhibiting dual emission colors. The orange stripes, which correspond to the TCNB–NAP–PY CT complex, formed selectively on the cleaved facets of TCNB–NAP CT microtubules exhibiting blue emission. b) PL spectra of (i) TCNB–NAP homogeneous microtubules, (ii) TCNB–NAP–PY homogeneous microtubules, and (iii) TCNB–NAP–PY heterogeneous microtubules. c) Fluorescence microscope image of a TCNB–NAP–PY heterogeneous microtubule, and d) its corresponding filtered fluorescence microscopy image (λ_{cutoff} = 520 nm). e) Fluorescence microscope image of TCNB–NAP–PNT hetero-microtubules and f) the corresponding filtered fluorescence microscopy image. g) Fluorescence microscope image of TCNB–NAP–9MA hetero-microtubules and h) the corresponding filtered fluorescence microscopy image.

After detaching the mold, we finally obtained TCNB–NAP microtubule patterns by removing the residual NAP by sublimation. Because of the applied axial strain, numerous cracks were formed on the TCNB–NAP microtubules. Both fluorescence microscopy and SEM images clearly showed the formation of cracks on the microtubules (Figure 1c). The bright stripes on the microtubules in the fluorescence microscope image (Figure 1c) indicate that the light guided by the tubular structure of the TCNB–NAP CT complex leaks out at the cleaved edges. The cracks were almost perpendicular to the pattern axis, and the size of gap was in the 0–600 nm range.

The cleaved facets provided the active sites for doping and growth of the secondary CT complexes.[13] After creating cracks on TCNB–NAP microtubules, we subsequently exposed the samples to the vapor of secondary aromatic hydrocarbon compounds, including PY, 9MA, and PNT. No additional TCNB was supplied during the formation of the secondary CT complexes. When the vapor concentration and the deposition time were carefully optimized, secondary CT complexes were formed selectively at the cracks. To synthesize the TCNB–NAP–PY hetero-microtubules, we placed the glass slide patterned with TCNB–NAP microtubules beside a glass slide coated with a thin film of PY in a chamber and then heated them at 60 °C for 90 min. After the sample cooled to room temperature, the sample was gently purged with argon. In contrast to the previous *in situ* doping of TCNB–NAP microtubules with PY, the microtubules prepared by this *ex situ* doping method exhibited orange stripes on the blue microtubules in the fluorescence microscope image (Figures 2a and c–d). The orange stripes, which suggest the formation of TCNB–NAP–PY CT complex, were exclusively observed where cracks were originally located. The filtered fluorescence microscope images more clearly show that the TCNB–NAP microtubules were heterogeneously doped with PY (Figures 2c–d). The PL spectrum of the TCNB–NAP–PY hetero-microtubules exhibited two broad bands at ~490 and ~560 nm, which correspond to the emission bands of the TCNB–NAP and TCNB–NAP–PY CT complexes, respectively (Figure 2b). These results strongly suggest that the TCNB–NAP–PY hetero-microtubules were formed by selective doping of PY at the cracks in the TCNB–NAP microtubules. Similarly, TCNB–NAP-PNT and TCNB–NAP–9MA hetero-microtubules were prepared by doping TCNB–NAP microtubules with PNT and 9MA respectively (Figure 2e-h). The filtered fluorescence microscope images of the TCNB–NAP–PNT and TCNB–NAP–9MA hetero-microtubules also showed well-defined discrete green (λ_{max} = 553 nm) and red stripes (λ_{max} = 599 nm), respectively, which suggests the formation of TCNB–NAP–PNT and TCNB–NAP–9MA CT complexes at the cracks. The SEM images also demonstrated that the secondary CT complexes were selectively formed at the cracks (Figure 3). Interestingly, the microtubule fragments separated by the cracks were welded by filling the gaps with the secondary CT complexes.

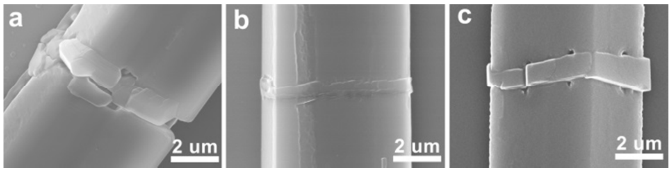

Figure 3. SEM images of a) a TCNB–NAP–PY hetero-microtubule, b) a TCNB–NAP–PNT hetero-microtubule, and c) a TCNB–NAP–9MA hetero-microtubule.

After the TCNB–NAP microtubules were doped with a certain aromatic dopant, they could be sequentially doped with other aromatic dopants. In this case, the sequential doping also occurred exclusively at the cracks; in addition, the apparent color changed to longer wavelengths when the second dopant had a HOMO level higher than that of the first dopant. For example, the TCNB–NAP microtubule containing cracks was first doped with PNT. The filtered microscope image shows that the TCNB–NAP–PNT CT complex, which exhibited green emission, was formed exclusively at the cracks (Figure 4b). When the TCNB–NAP–PNT hetero-microtubule was further exposed to the vapor of 9MA, which has a HOMO level slightly higher than that of PNT, the green emission bands turned to red, whereas other regions were unchanged (Figure 4c). Similarly, the green bands became orange when the TCNB–NAP–PNT hetero-microtubule was exposed to the vapor of PY. In contrast, no color change was observed for the opposite doping order. When the TCNB–NAP microtubules were doped first with 9MA, the red emission bands of the TCNB–NAP–9MA CT complex were unchanged after the complex was doped with PNT under the same experimental conditions. These results suggest that the charge transfer in microtubules occur dominantly between the TCNB and a dopant having the highest HOMO level. The general trend of fluorescence peak shift by the secondary doping is well consistent with this argument. The HOMO levels of dopants are in the order of NAP (–8.14 eV),[16] PNT (–7.90 eV),[17] PY (–7.40 eV),[18] and 9MA (–7.27 eV).[19]

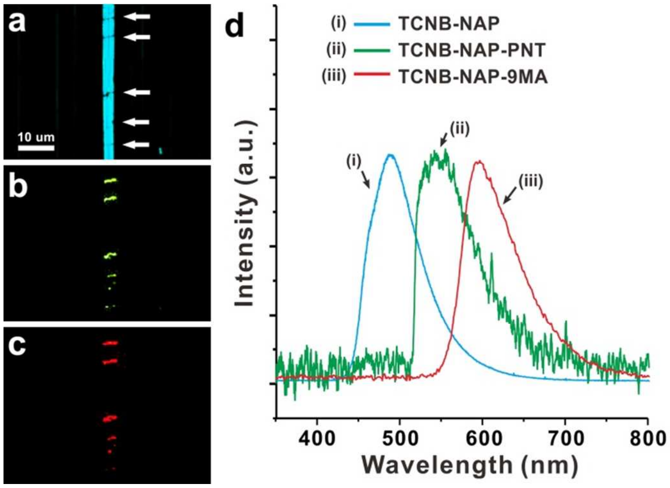

Figure 4. Sequential doping of a TCNB–NAP microtubule with different dopants. a) A fluorescence confocal microscopy image of a TCNB–NAP microtubule. b) A filtered fluorescence confocal microscope image of a TCNB–NAP–PNT hetero-microtubule that was prepared by doping a TCNB–NAP microtubule with PNT (λ_{cutoff} = 510 nm). c) Filtered fluorescence confocal microscope image of a TCNB–NAP–PNT–9MA hetero-microtubule that was prepared by doping a TCNB–NAP–PNT hetero-microtubule with 9MA (λ_{cutoff} = 510 nm). d) PL spectra obtained from (i) image a, (ii) image b, and (iii) image c.

In summary, we have presented an approach to fabricating dual-color-emitting organic hetero-microtubules consisting of multi-segments of two different CT complexes. Our "crack-welding" method exploits the selective doping and growth of the secondary CT complexes at the cracks of TCNB–NAP CT microtubules. Eutectic-melting-assisted soft-lithography was adopted for creating the cracked TCNB–NAP CT microtubules by applying axial strain to a PDMS mold. Because of the relatively high reactivity of the cleaved facets of the TCNB–NAP CT microtubules, the secondary CT complexes were selectively grown at the positions of the original cracks when the microtubules were exposed to the vapor of aromatic hydrocarbon dopants, including PY, PNT, and 9MA. The sequential doping in the sequence of increasing HOMO level of the aromatic dopants led to serial shifts of the emission color of the hetero-microtubules to a longer wavelength. We anticipate that our method can be easily applied to the creation of various heterogeneous structures based on CT complexes.

This work was supported by the National Research Foundation of Korea (NRF) grant funded by the Korea government (2011-0017197), NRF (2012M2A2A6035933) and by Basic Science Research Program through the National Research Foundation of

Korea (NRF) funded by the Ministry of Education (2012R1A6A1029029).

Notes and references

[a] Department of Chemistry, Research Institute for Natural Sciences, and Institute of Nano Science and Technology, Hanyang University, 222 Wangsimni-Ro, Seongdong-Gu, Seoul, 133-791 (Korea).

Electronic Supplementary Information (ESI) available: [details of any supplementary information available should be included here]. See DOI: 10.1039/c000000x/

1 (a) X. Feng, G. Hu and J. Hu, *Nanoscale*, 2011, **3**, 2099; (b) R. Costi, A. E. Saunders and U. Banin, *Angew. Chem. Int. Ed.*, 2010, **49**, 4878; (c) C. Wang, C. Xu, H. Zeng and S. Sun, *Adv. Mater.*, 2009, **21**, 3045; (d) P. D. Cozzoli, T. Pellegrino and L. Manna, *Chem. Soc. Rev.*, 2006, **35**, 1195; (e) M. R. Buck, J. F. Bondi and R. E. Schaak, *Nature chemistry*, 2012, **4**, 37; (f) J. Yuan, Y. Xu and A. H. Müller, *Chem. Soc. Rev.*, 2011, **40**, 640; (g) C.-H. Hsieh, L.-J. Chou, G.-R. Lin, Y. Bando and D. Golberg, *Nano Lett.*, 2008, **8**, 3081; (h) J. Li and J. Z. Zhang, *Coord. Chem. Rev.*, 2009, **253**, 3015.

2 (a) J. Yang, H. I. Elim, Q. Zhang, J. Y. Lee and W. Ji, *J. Am. Chem. Soc.*, 2006, **128**, 11921; (b) T. Mokari, C. G. Sztrum, A. Salant, E. Rabani and U. Banin, *Nat. Mater.*, 2005, **4**, 855.

3 E. Elmalem, A. E. Saunders, R. Costi, A. Salant and U. Banin, *Adv. Mater.*, 2008, **20**, 4312.

4 (a) R. Costi, A. E. Saunders, E. Elmalem, A. Salant and U. Banin, *Nano Lett.*, 2008, **8**, 637; (b) P. Li, Z. Wei, T. Wu, Q. Peng and Y. Li, *J. Am. Chem. Soc.*, 2011, **133**, 5660; (c) Y. Shemesh, J. E. Macdonald, G. Menagen and U. Banin, *Angew. Chem.*, 2011, **123**, 1217.

5 (a) T. Mokari, E. Rothenberg, I. Popov, R. Costi and U. Banin, *Science*, 2004, **304**, 1787; (b) M. A. Bangar, C. M. Hangarter, B. Yoo, Y. Rheem, W. Chen, A. Mulchandani and N. V. Myung, *Electroanalysis*, 2009, **21**, 61; (c) Y. Zhang, H. Dong, Q. Tang, S. Ferdous, F. Liu, S. C. Mannsfeld, W. Hu and A. L. Briseno, *J. Am. Chem. Soc.*, 2010, **132**, 11580.

6 X. Guo, M. Qiu, J. Bao, B. J. Wiley, Q. Yang, X. Zhang, Y. Ma, H. Yu and L. Tong, *Nano Lett.*, 2009, **9**, 4515.

7 (a) S. Selvan, P. K. Patra, C. Y. Ang and J. Y. Ying, *Angew. Chem.*, 2007, **119**, 2500; (b) C. Xu, J. Xie, D. Ho, C. Wang, N. Kohler, E. G. Walsh, J. R. Morgan, Y. E. Chin and S. Sun, *Angew. Chem. Int. Ed.*, 2008, **47**, 173; (c) J.-s. Choi, Y.-w. Jun, S.-I. Yeon, H. C. Kim, J.-S. Shin and J. Cheon, *J. Am. Chem. Soc.*, 2006, **128**, 15982; (d) A. Figuerola, A. Fiore, R. Di Corato, A. Falqui, C. Giannini, E. Micotti, A. Lascialfari, M. Corti, R. Cingolani and T. Pellegrino, *J. Am. Chem. Soc.*, 2008, **130**, 1477.

8 (a) S. E. Habas, P. Yang and T. Mokari, *J. Am. Chem. Soc.*, 2008, **130**, 3294; (b) H. Yu, M. Chen, P. M. Rice, S. X. Wang, R. White and S. Sun, *Nano Lett.*, 2005, **5**, 379; (c) W. Zhang, W. Jin, T. Fukushima, A. Saeki, S. Seki and T. Aida, *Science*, 2011, **334**, 340.

9 (a) C. R. Martin, DTIC Document, 1994; (b) S. R. Nicewarner-Pena, R. G. Freeman, B. D. Reiss, L. He, D. J. Peña, I. D. Walton, R. Cromer, C. D. Keating and M. J. Natan, *Science*, 2001, **294**, 137; (c) S. Park, J.-H. Lim, S.-W. Chung and C. A. Mirkin, *Science*, 2004, **303**, 348; (d) D. J. Pena, J. K. Mbindyo, A. J. Carado, T. E. Mallouk, C. D. Keating, B. Razavi and T. S. Mayer, *J. Phys. Chem. B*, 2002, **106**, 7458.

10 (a) B. Sadtler, D. O. Demchenko, H. Zheng, S. M. Hughes, M. G. Merkle, U. Dahmen, L.-W. Wang and A. P. Alivisatos, *J. Am. Chem. Soc.*, 2009, **131**, 5285; (b) D. H. Son, S. M. Hughes, Y. Yin and A. P. Alivisatos, *Science*, 2004, **306**, 1009; (c) P. H. Camargo, Y. H. Lee, U. Jeong, Z. Zou and Y. Xia, *Langmuir*, 2007, **23**, 2985; (d) J. M. Pietryga, D. J. Werder, D. J. Williams, J. L. Casson, R. D. Schaller, V. I. Klimov and J. A. Hollingsworth, *J. Am. Chem. Soc.*, 2008, **130**, 4879.

11 R. D. Robinson, B. Sadtler, D. O. Demchenko, C. K. Erdonmez, L.-W. Wang and A. P. Alivisatos, *Science*, 2007, **317**, 355.

12 Y. L. Lei, L. S. Liao and S. T. Lee, *J. Am. Chem. Soc.*, 2013, **135**, 3744.

13 P. Gumbsch and R. M. Cannon, *MRS Bull.*, 2000, **25**, 15.

14 (a) M. Koz'menko and M. Kuz'min, *J. Appl. Spectrosc.*, 1977, **27**, 1129; (b) Y.-L. Lei, Y. Jin, D.-Y. Zhou, W. Gu, X.-B. Shi, L.-S. Liao and S.-T. Lee, *Adv. Mater.*, 2012, **24**, 5345; (c) N. Mataga and Y. Murata, *J. Am. Chem. Soc.*, 1969, **91**, 3144; (d) R. J. Dillon and C. J. Bardeen, *J. Phys. Chem. A*, 2011, **115**, 1627.

15 S. Iwata, J. Tanaka and S. Nagakura, *J. Am. Chem. Soc.*, 1967, **89**, 2813.

16 M. C. Cockett, H. Ozeki, K. Okuyama and K. Kimura, *The Journal of chemical physics*, 1993, **98**, 7763.

17 N. Thantu and P. M. Weber, *Chem. Phys. Lett.*, 1993, **214**, 276.

18 E. Clar, J. Robertson, R. Schlögl and W. Schmidt, *J. Am. Chem. Soc.*, 1981, **103**, 1320.

19 C. Jongsma, H. Vermeer, F. Bickelhaupt, W. Schäfer and A. Schweig, *Tetrahedron*, 1975, **31**, 2931.